Key Engineering Materials Vols. 554-557 (2013) pp 2054-2061
© (2013) Trans Tech Publications, Switzerland
doi:10.4028/www.scientific.net/KEM.554-557.2054

3D Simulation of Laser Assisted Side Milling of Ti6Al4V Alloy using Modified Johnson-Cook Material Model

Hassan Zamani[1, a], Jan-Patrick Hermani[2, b] Bernhard Sonderegger[3, c] and Christof Sommitsch[4, d]

[1]Institute for Materials Science and Welding, Graz University of Technology, Kopernikusgasse 24/I, Graz 8010, Austria

[2] Fraunhofer Institute for Production Technology IPT, Steinbachstrasse 17, 52074 Aachen, Germany

[3]Institute for Materials Science and Welding, Graz University of Technology, Kopernikusgasse 24/I, Graz 8010, Austria

[4]Institute for Materials Science and Welding, Graz University of Technology, Kopernikusgasse 24/I, Graz 8010, Austria

[a]hassan.zamani@tugraz.at, [b]jan-patrick.hermani@ipt.fraunhofer.de, [c]bernhard.sonderegger@tugraz.at, [d]christof.sommitsch@tugraz.at

Keywords: Cutting Forces, FEM, Laser Assisted Machining, Side Milling, Ti-6Al-4V

Abstract. During machining of hard materials, one approach to reduce tool wear is using a laser beam to preheat the material in front of the cutting zone. In this study, a new concept of laser-assisted milling with spindle and tool integrated laser beam guiding has been tested. The laser beam is located at the cutting edge and moving synchronously with the cutter. In experiment, a reduction in the resulting process cutting forces and tool wear has been observed in comparison to milling without laser. A three-dimensional finite element model in DEFORM 3D was developed to predict the cutting forces in the milling process with and without an additional laser heat source, based on a Johnson-Cook-type material constitutive model adapted for high strains and strain rates. Both in experiment and simulation, the deformation behavior of a Ti-6Al-4V workpiece has been investigated. The comparison of the resulting cutting forces showed very good agreement. Thus the new model has great potential to further optimize laser assisted machining processes.

Introduction

Today, still more than 50% of titanium products are based on the alloy Ti-6Al-4V, indicating the importance of this material in various industries, reaching from aerospace to sport. The reason can be found in the unique profile of this alloy, which at a glance flaunts high strength (even at temperatures up to 400°C), light weight and corrosion resistance. But, what in the meantime restricts the application of this alloy is the processing, which places Ti-6Al-4V on the list of hard-to-machined materials. In other words, machining of Titanium is expensive due to high tool wear, and the productivity is low due to limited cutting speed [1]. To overcome these difficulties, heating the material and according material softening could be a solution and obviously, the heat input management a necessity. However, merciful heating, regardless of energy costs, can lead to defects such as hot crack susceptibility, microstructure transformation and formation of oxide layer in the machined part. One option to overcome these difficulties is local heating in front of the cutting zone using a laser beam. Laser-assisted-machining has been investigated for 30 years [2] and induces softening effects leading to a reduction of tool wear. This goal was achieved, but absence of the modular and scalable tool systems with integrated optics as one single equipment without any peripheral device for laser-assisted machining is felt. In this line, Fraunhofer IPT has taken the first steps with introducing new process concept [3]. The main difference between the novel system and common laser-assisted milling is the position of the laser spot: contrary to conventional systems, the conducted laser beam is placed directly on the cutting surface through the rotating machine spindle using an embedded mirror. Along these practical efforts, a thermo-mechanical process model for the laser assisted machining of high strength metallic and ceramic materials has been set up, saving time consuming and expensive testing periods. For this purpose, a finite element model (FEM) was developed to predict the required process parameters for different materials, operation modes and components geometries. Such a model is highly desired by respective end users and will be helpful to optimize any laser-assisted cutting process such as milling and turning.

Experimental Setup

The experiments were performed on a Satisloh G1 3+2 axis machining center with Bosch Rexroth MTX P60 NC control and with optical and mechanical interfaces which integrated into the spindle, see figure 1. The process gas is supplied over a rotary lead through interface on the spindle housing which is tied to the collimation (collimating lens). The process gas protects the optical lens and mechanical components from the overheating. Furthermore, the process gas pushes away the dispersed chips from the optical lens and the beam path, which supports the thermal process efficiency. An IPG YLR high fiber laser (Yb: YAG with a wavelength of 1070 mm) with maximum power of 6 KW, was applied to the laser radiation. The diverging laser beam is changed into a nearly parallel beam by an aspheric collimating lens and transits through the spindle with hollow shaft. A tool integrated focusing system converts the delivered beam into the converging laser beam which is projected by two high reflection mirrors directly on the cutting surface edge in front of the cutting insert. In order to prevent the radiation of laser beam on the finished surface, the laser power is switched on/off at entrance and exit points, receptively. The laser power is modified according the uncut chip thickness during one revolution in the milling process. All the experiments was performed with round inserts (RDHX 07 07 MOT D*D1*S- 7*2.7*2.38 with the rake angle 11 °) at a fixed depth of cut of 0.5 mm using TiAlN-coated cemented carbide. The maximum laser power varied from 0 to 1428 W, while the laser spot diameter was 1 mm. The fix distance between insert and the center of laser spot (arc length) is 5 mm. Furthermore, the trials was conducted at different cutting velocity and feed rate with a mill diameter 24 mm and the cutting width 8 mm. The workpiece material was forged Ti-6Al-4V in annealed, pickled and stress relieved condition. During the machining experiments, a piezo-based three dimensional force measurement, determined the process forces in 3 directions. For one path of milling, the maximum forces in each revolution (with the frequent of 200 up to 450 kHz) were averaged. Flank wear analyses were based on the microscopic investigation.

Experimental results

Effect of cutting velocity on the force reduction. Figure 2 illustrates the effect of cutting velocity on the cutting forces for feed rates 70 and 90 µm/rev with laser (laser power: 1250 W) and without laser. With increasing the velocity, the heat generation due the friction at the interface area increases, which leads to the velocity-caused softening of the workpiece and consequently a reduction in the main cutting force (F_Y). This effect is more remarkable, as the cutting velocity exceed the velocities near to the 150 m/min. In order to keep the accuracy of the force measurement, the tests was performed in the cutting velocities up to 125 m/min. However, in the laser assisted milling, with increasing the cutting velocity, time for the heat transfer will shorter, hence, the cutting force reduction decreases, but the cutting forces are less than the milling without laser.

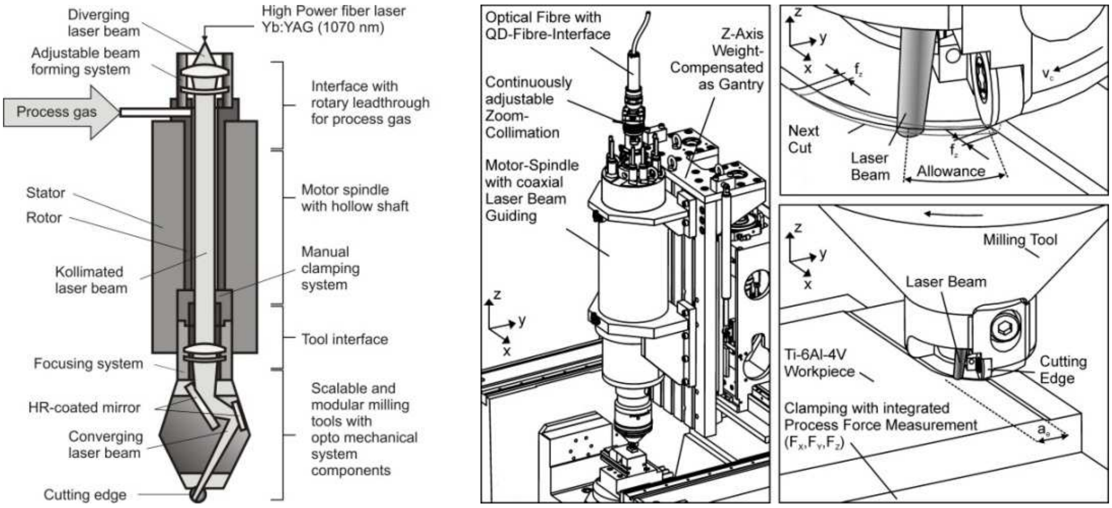

Figure 1. The working principle of the novel laser-assisted-milling [3].

Effect of laser power on the force reduction. Figures 3 shows the effect of laser power on the three components of forces at two different milling speeds (25 and 50 m/min). Generally, with increasing the laser power, the forces are decreased. However, the reduction of forces is more significant in the Z and Y direction. Furthermore, the experimental results show the reduction of main cutting force (F_Y) more pronounced than the force normal to the milling surface (F_Z). The reason of the smaller reduction of forces in Z direction can be found in the sticking of chip on the tool tip at the low feed rates. As it can be seen in Figures 3, the reduction of (F_Z) goes into uniformly with increasing the feed rate and also cutting velocity. The influence of laser power on the forces in the feed direction is also small. These forces are more sensitive into the feed rate.

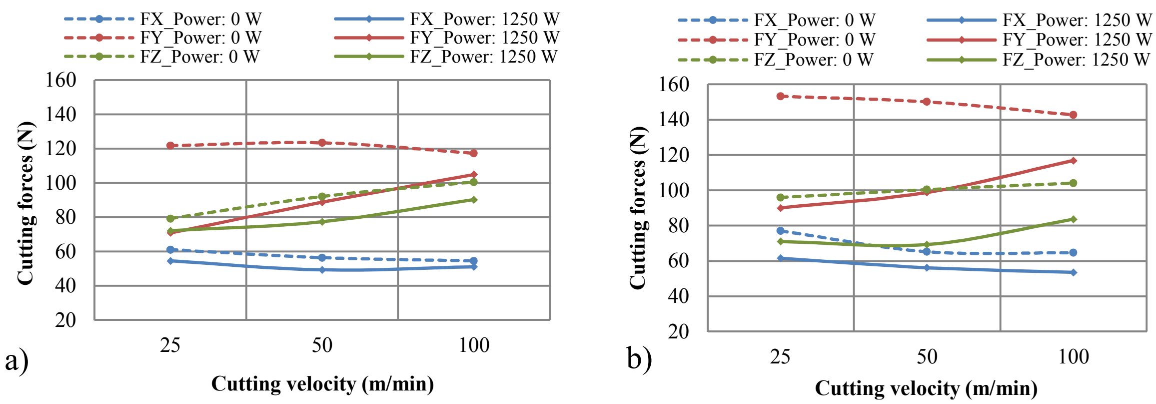

Figure 2. The effect of cutting velocity on cutting forces (a) feed rate 70 and (b) 90 µm/rev.

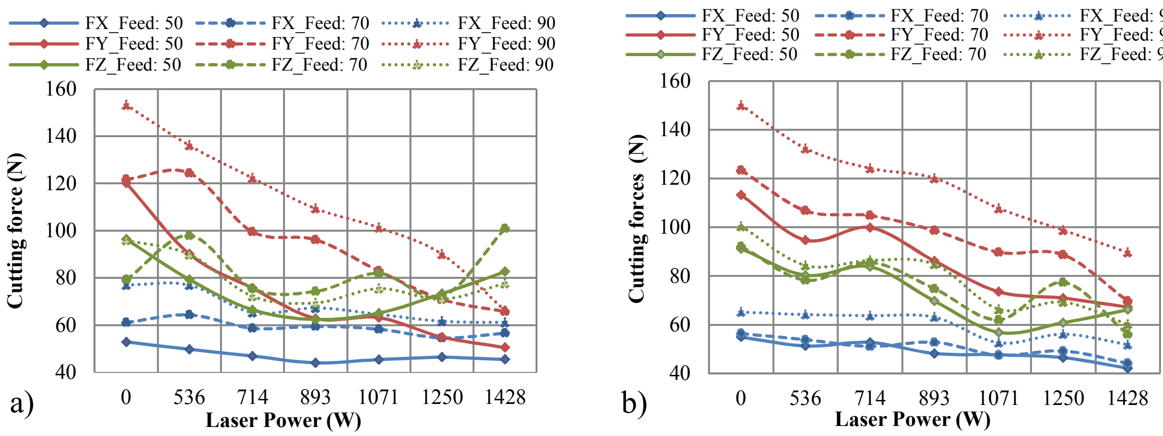

Figure 3. The effect of laser power on cutting forces (a) cutting velocity 25 and (b) 50 m/min.

Effects of tool wear on the force reduction. Figures 4 (a) and 5 (a) show the resulting forces based on the material removal volume for the side milling process with /without laser (cutting velocity: 57 m/min, feed rate: 80 µm/rev, laser power: 900 W). It can be seen that the forces (main influence is on F_Y and F_Z) increase with the time in both processes, but the slope of force increase is lower in case of the laser assisted milling. The reason can be explained with the change of the tool tip shape (from sharp into round) which changes the stress and the contact area. Figures 3 (b) and 4 (b) illustrate the final tool tip geometry after the milling processes, which confirm a reduction of tool wear in case of milling with laser.

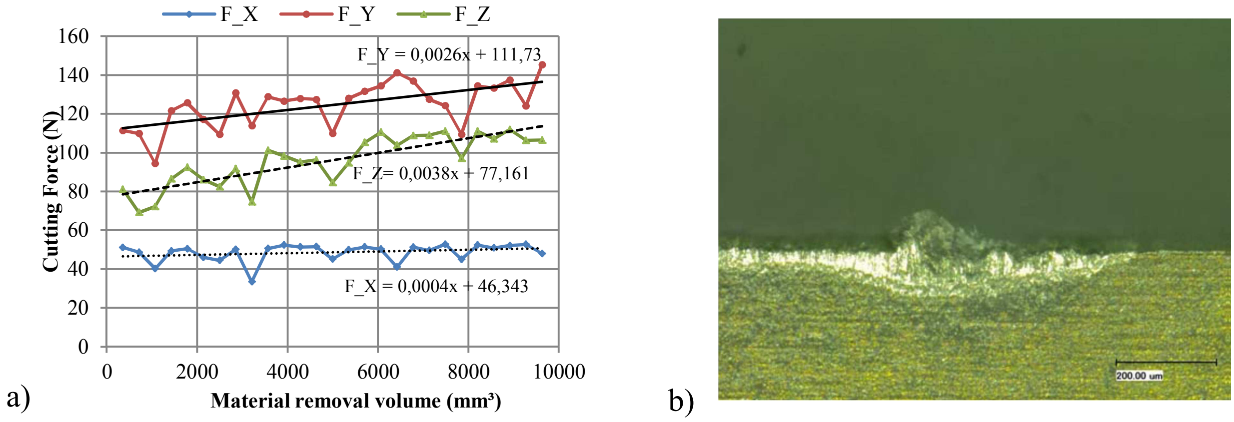

Figure 4. (a) The effect of milling time on the processes forces without laser (b) flank wear appearance at the end of milling process.

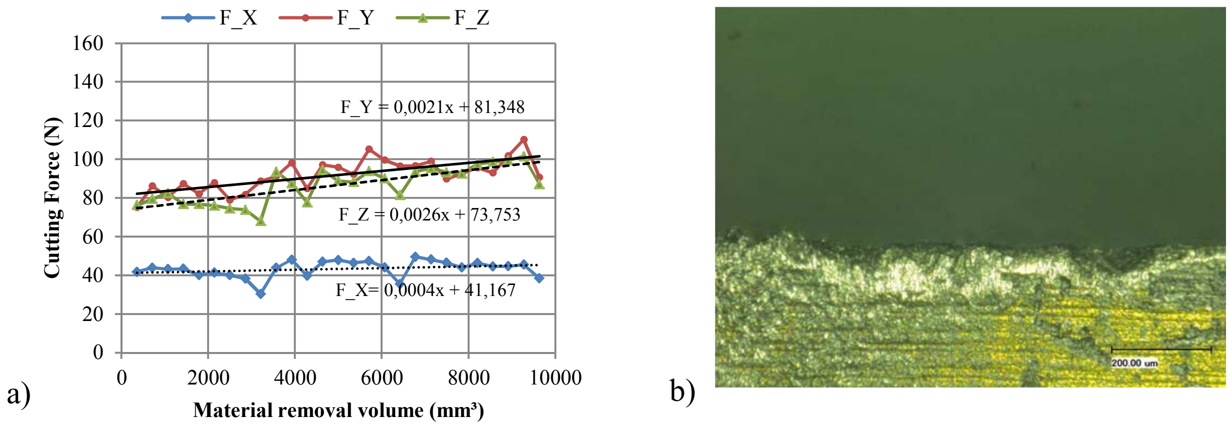

Figure 5. (a) The effect of milling time on the process forces with laser (b) flank wear appearance at the end of milling process.

3-D FEM Simulation

The commercial software DEFORM 3D has been used to set up a thermo-mechanical FEM model for the laser assisted machining process. The thermo-physical properties and cutting conditions used in the simulations are indicated in Table 1. Based on the Zorev's model [6], the tangential shear stresses on the tool surface cannot exceed the yield shear stress of chip material. The following relations express the frictional condition at the tool-chip interface:

$$\tau = \mu\sigma_n, \qquad \text{if} \qquad \mu\sigma_n < \bar{m}\frac{\sigma_{eq}}{\sqrt{3}}$$
$$\tau = \bar{m}\frac{\sigma_{eq}}{\sqrt{3}}, \qquad \text{if} \qquad \mu\sigma_n \geq \bar{m}\frac{\sigma_{eq}}{\sqrt{3}} \qquad (1)$$

where σ_n is normal stress, τ is shear stress, σ_{eq} is the equivalent flow stress, μ is Coulomb friction coefficient and $\bar{m}$ is shear factor.

Material model. Recently, a modified Johnson-Cook material model has been set up by Calamaz and Sima [7, 8, 9]. The modifications consider the strain softening which is defined as decreasing the flow stress with increasing strain over a critical strain value. This strain decreasing is justified by the dynamic recovery and/or recrystallization which lead to rearrangement of dislocations. The modified model helps to predict better saw-tooth chip formation in titanium alloys.

Table 1. Input data used in FEM analysis.

Material	Modified Johnson- Cook material law		Ti6Al4V	
	Inelastic heat fraction		0.9	
	Conductivity (W/mK)	Workpiece (Ti6Al4V) [4]	25	7
			500	12.6
			900	20.2
			995	19.3
			1100	21
			1650	28.4
		Tool (TiAlN-coated cemented carbide) [5]	25	12
			1000	20
	heat capacity (J/Kg K)	Workpiece (Ti6Al4V) [4]	25	546
			500	651
			900	734
			995	641
			1100	660
			1650	759
		Tool (TiAlN-coated cemented carbide) [5]	598	
Contact area	heat transfer coefficient (kW/m²K)		50	
	Heat partition coefficient		0.6	
	Friction coefficient		$\bar{m}$= 0.7 μ= 0.5	
	Friction energy transformed into heat		1	
Environment	Forced convection (Air jet cooling, Overhead) (W/m²K)		2000	
Milling conditions	Cutter		RDHX 0702 MOT	
	Cutting width(mm)		8	
	Rake angle (°)		11	
	Nose radius(mm)		0.02	
	Depth of cut (mm)		0.5	
	Cutting velocity(m/min)		25, 50, 75, 100	
	Rotation velocity of tool (rpm)		332, 663, 995, 1326	
	Feed (mm/rev)		0.05, 0.07, 0.09	
	Laser power (W)		536, 714, 893, 1071, 1250, 1428	

The reason can be explained with a hidden failure model (but here instead of update the value of stress components equal to zero, the stresses decreases continuously) with a critical strain value. The achieved chip morphology in 3D simulation is shown in Figure 6 (b). It should be mentioned, the remarkable chip serration can be realized in 2D simulation with finer element size.

$$\sigma_{eq} = \left(A + \frac{B\varepsilon^n}{\exp(\varepsilon^a)}\right)\left(1 + C\ln\left(\frac{\dot{\varepsilon}}{\dot{\varepsilon}_0}\right)\right)\left(1 - \left(\frac{T - T_r}{T_m - T_r}\right)^m\right)\left(D + (1 - D)\left[\tanh\left(\frac{1}{(\varepsilon + S)^c}\right)\right]^e\right) \quad (3)$$

where $D = 1 - \left(\frac{T}{T_m}\right)^d$, $p = \left(\frac{T}{T_m}\right)^b$. The effect of the constants on the flow curve is listed in Table 2.

Table 2. Effect of Material Constants of the Modified JC-Model on the Flow Stress Curves

Modified JC model parameters	Effect on the flow stress curve
S	Decreasing the critical strain value depending temperature
D	Decreasing the flow stress at the high strains depending temperature
a	Slope of the flow stress decreasing after the critical strain value at high strains
b	Position of maximum flow stress (critical strain value)
c	Slope of the flow stress decreasing after the critical strain value at low strains
d	Magnitude of strain softening

The material model constants for both models are listed in Table 3:

Table 3. Material constants

	A (MPa)	B (MPa)	C	m	n	T_m (°C)	a	b	c	d	e
Modified JC-model [8]	724	683.2	0.035	1.0	0.47	1660	2	1	2	1	0.05

Thermal modeling. With the purpose of predicting the temperature field at the workpiece subjected with the laser beam, a 3D moving laser heat source model with respect to the natural boundary condition and temperature depending thermo-physical material properties was developed. During the movement of the laser spot, a maximum steady temperature is approached, depending on laser parameters, material properties and absorption coefficient. In order to inset the laser power intensity as the input parameter, the local convection coefficient approaches to near zero. The model enables to investigate the effect of laser power, laser spot size, and distance between insert and laser spot incident angle, rotation velocity and feed velocity on the resulting temperature field. Also, it is possible to vary the laser power during one revolution of mill according to the chip thickness. A laser absorption coefficient of 27 % was calculated based on the formation of melting surface during one rotation of mill by a number of tests with varying laser power and constant rotation velocity.

Simulation Results and Model Validation

Analogous to the experimental trials, the maximum forces (corresponding to the maximum chip thickness) in 3D FEM simulation was calculated. The simulation results were compared with the experimental results in the different milling conditions with and without laser. The forces were calculated until an absolute maximum value was achieved; then the simulation went into the steady state for further temperature calculation.

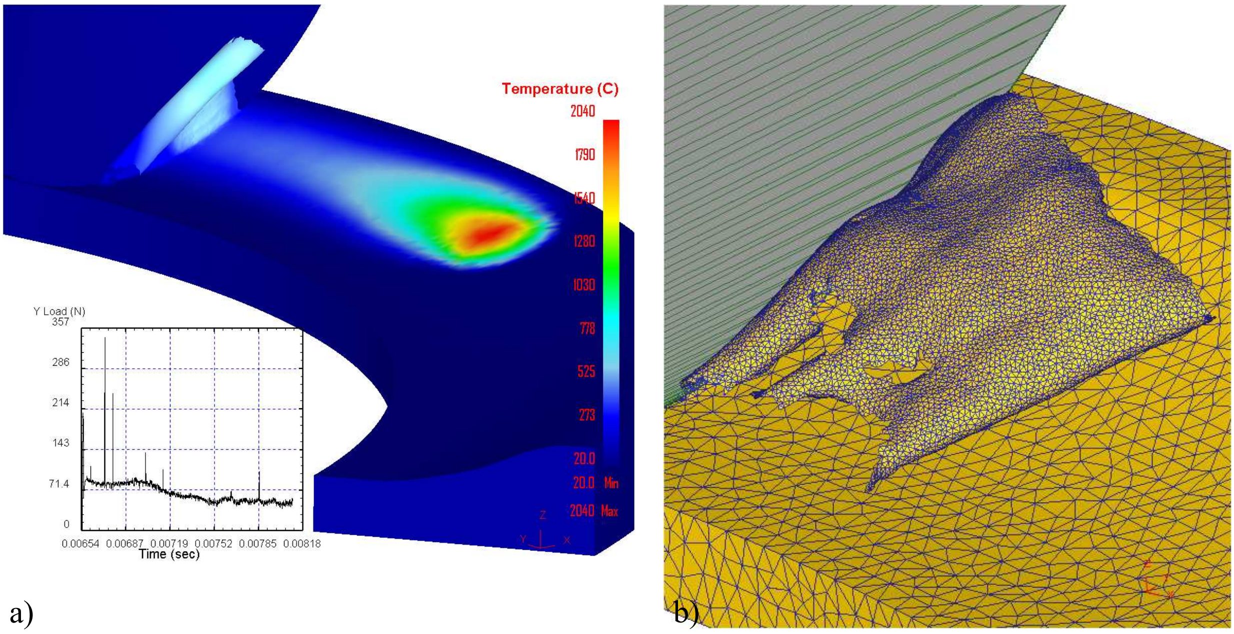

Figure 6. (a) 3D FEM model of laser-assisted-side milling process (b) chip formation using modified JC-model.

Figure 7 shows comparison between the cutting forces from simulation and experimental results. Without laser, the simulation results showed lower values (up to 10%) of forces in machining compared to experiments. With laser powers of 1071 W and above, forces in Z-direction are about 10 % higher in simulation compared to experiments. The reason may be justified in temperature dependence of the thermal softening constant n. The forces in X-direction are generally underestimated in the simulation. Overall, the agreement between simulated and experimental results is very good and mostly within experimental scattering.

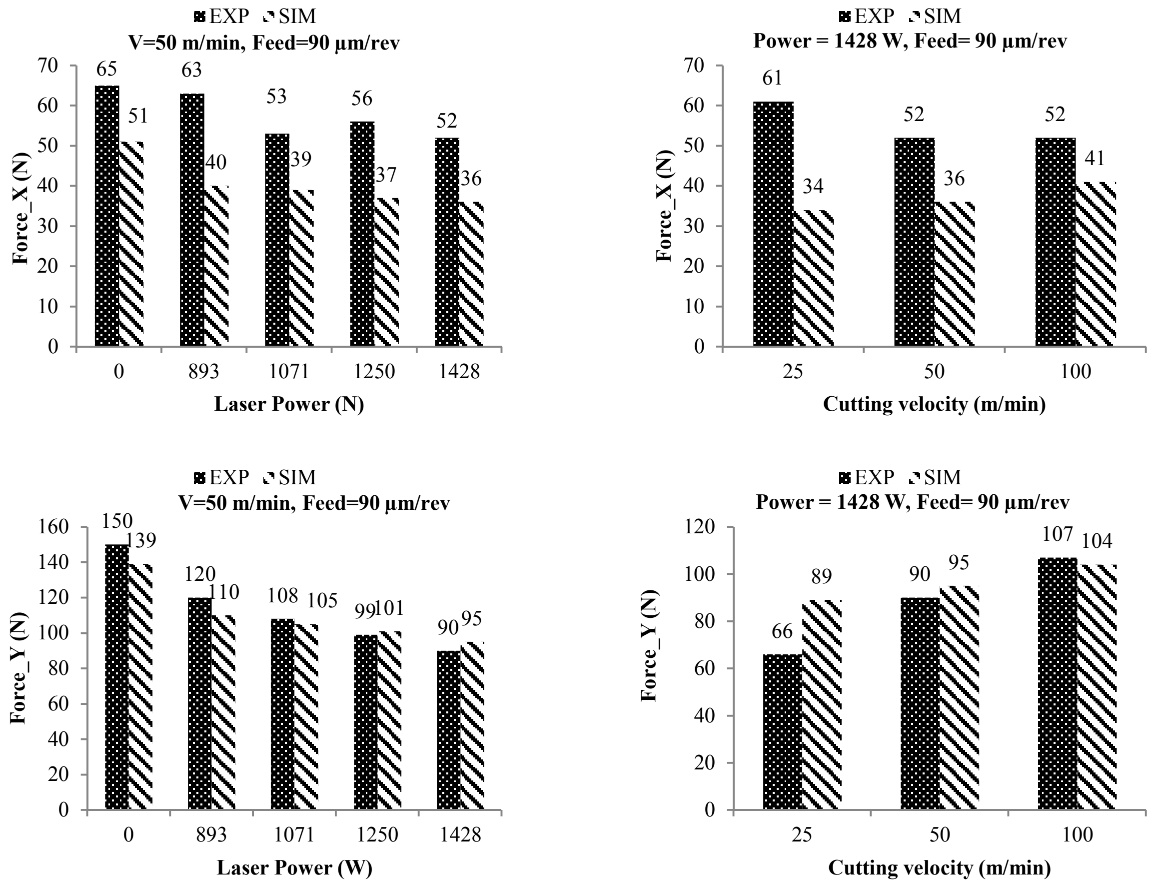

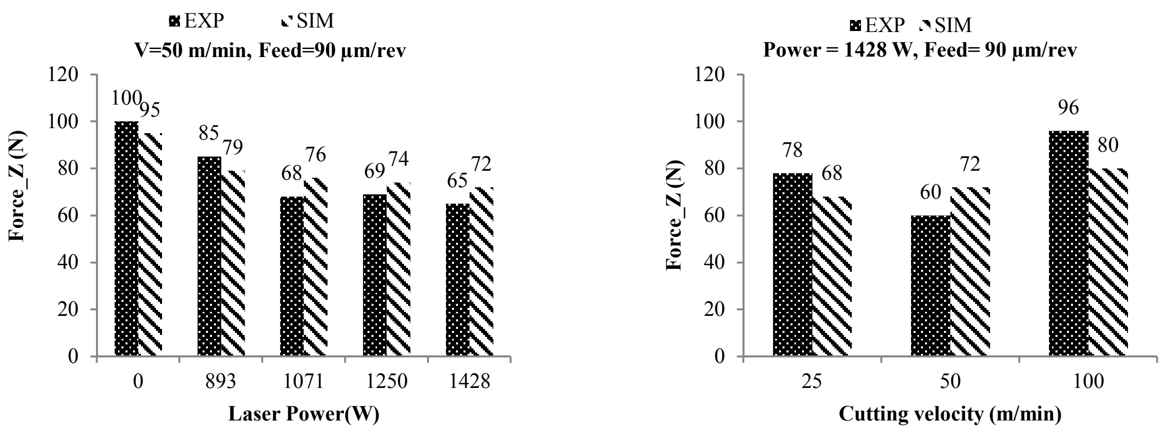

Figure 7. Comparison between simulation and experimental milling forces at the different milling conditions.

Summary

In this study, the results of laser-assisted milling of Ti-6Al-4V using TiAlN-coated cemented carbide cutting insert in different cutting conditions are presented. A significant reduction of forces was achieved with the optimization of the machining and laser parameters. The results showed a reduction of force in X-direction up to 25%, Y-direction up to 60% and Z-direction up to 65%. Furthermore, the tool wear could be reduced significantly by the assistance of the laser, resulting in an increased tool life. Beside the experimental investigations, the effects of varying process parameters were studied within a 3D-FEM simulation. The results showed very good agreement between simulated and experimentally found cutting forces in all directions. Thus the simulation lays a solid basis for further optimizing the process parameters for reduced cutting forces and tool wear.

References

[1] W. König, A. Zaboklicki, Laserunterstützte Drehbearbeitung von Silizium-Nitrid-Keramik, VDI-Z 135, 6 (1993), 34-39.

[2] E. O. Ezugwu, Z. M. Wang, Titanium alloys and their machinability—a review, Journal of Materials Processing Technology, 68 (1997), 262–274.

[3] C. Brecher, M. Emonts, C. J. Rosen and J. P. Hermani, Laser-assisted Milling of Advanced Materials, Physics Procedia, 12 (2011), 599-606.

[4] K. C. Mills, Recommended Values of Thermo physical Properties for Selected Commercial Alloys, Woodhead Publishing (2002), 217.

[5] Deform-User Manual SFTC-Deform V10.0.2, Columbus (OH), USA, (2010).

[6] N. Zorev, Inter-relationship between shear processes occurring along tool face and shear plane in metal cutting, International Research in Production Engineering, 1963, 42-49.

[7] M. Calamaz, D. Coupard, F. Girot, A New Material Model for 2D Numerical Simulation of Serrated Chip Formation when Machining Titanium Alloy Ti–6Al–4V, International Journal of Machine Tools & Manufacture,48 (2008), 275–288.

[8] M. Sima, T. Özel, Modified material constitutive models for serrated chip formation simulations and experimental validation in machining of titanium alloy Ti6Al4V, International Journal of Machine Tools and Manufacture 50 (2010), 943-960.

[9] D. Ulutan, M. Sima, T. Özel, Prediction of Machining Induced Surface Integrity using Elastic-Viscoplastic Simulations and Temperature-Dependent Flow Softening Material Models in Titanium and Nickel-based alloys, Advanced Materials Research, 223(2011), 401-410.